Epidemics 9 (2014) 18–30

Contents lists available at ScienceDirect

Epidemics

journal homepage: www.elsevier.com/locate/epidemics

Impacts of constrained culling and vaccination on control of foot and mouth disease in near-endemic settings: A pair approximation model

N. Ringa[a,*], C.T. Bauch[a,b]

[a] Department of Mathematics and Statistics, University of Guelph, 50 Stone Rd E, Guelph, ON N1G 2W1, Canada
[b] Department of Applied Mathematics, University of Waterloo, 200 University Avenue, West Waterloo, ON N2L 3G1, Canada

ARTICLE INFO

Article history:
Received 28 February 2014
Received in revised form
19 September 2014
Accepted 21 September 2014
Available online 28 September 2014

Keywords:
Foot and mouth disease
Pair approximation models
Vaccination
Culling
Constrained control

ABSTRACT

Many countries have eliminated foot and mouth disease (FMD), but outbreaks remain common in other countries. Rapid development of international trade in animals and animal products has increased the risk of disease introduction to FMD-free countries. Most mathematical models of FMD are tailored to settings that are normally disease-free, and few models have explored the impact of constrained control measures in a 'near-endemic' spatially distributed host population subject to frequent FMD re-introductions from nearby endemic wild populations, as characterizes many low-income, resource-limited countries. Here we construct a pair approximation model of FMD and investigate the impact of constraints on total vaccine supply for prophylactic and ring vaccination, and constraints on culling rates and cumulative culls. We incorporate natural immunity waning and vaccine waning, which are important factors for near-endemic populations. We find that, when vaccine supply is sufficiently limited, the optimal approach for minimizing cumulative infections combines rapid deployment of ring vaccination during outbreaks with a contrasting approach of careful rationing of prophylactic vaccination over the year, such that supplies last as long as possible (and with the bulk of vaccines dedicated toward prophylactic vaccination). Thus, for optimal long-term control of the disease by vaccination in near-endemic settings when vaccine supply is limited, it is best to spread out prophylactic vaccination as much as possible. Regardless of culling constraints, the optimal culling strategy is rapid identification of infected premises and their immediate contacts at the initial stages of an outbreak, and rapid culling of infected premises and farms deemed to be at high risk of infection (as opposed to culling only the infected farms). Optimal culling strategies are similar when social impact is the outcome of interest. We conclude that more FMD transmission models should be developed that are specific to the challenges of FMD control in near-endemic, low-income countries.

1. Introduction

Foot and mouth disease (FMD) is a highly contagious, and non-curable viral disease of economically important cloven-hoofed animals such as cattle, pigs, goats and sheep (Baipoledi et al., 2004; Keeling et al., 2001; Wernery and Kinne, 2012; Ferguson et al., 2001; Pharo, 2002), and more than 70 species of wild animals, e.g. deers, antelopes and buffaloes (Dion et al., 2011; Grubman and Baxt, 2004). The disease agent which causes FMD belongs to the *picorna* virus family (Belsham et al., 2011; Dion et al., 2011), and it exists in seven known immunologically distinct serotypes which vary according to world geographical location (Rweyemamu, 1984; Alonso et al., 1992): (a) European types O, A and C; (b) African types STA 1, STA 2 and STA 3 and (c) Asian type Asia 1 (Davies, 2002; Ding et al., 2013). The FMD virus serotypes are further divided into several (more than 60) subtypes (Alonso et al., 1992; Anderson et al., 1974; Belsham et al., 2011) and they all occur with little cross-protection between each other (Kitching et al., 2007). The virus is airborne and can also be transmitted through physical contact with infected animals' expired air, saliva, milk, urine, semen, animal feed and bedding, etc (Ferguson et al., 2001; Baipoledi et al., 2004; Grubman and Baxt, 2004). FMD is rarely fatal, but infected animals display high fever, depression, loss of weight and drop in milk production, as well as blisters on the tongue, lips, mouth, and between toes (Rweyemamu, 1984; Baipoledi et al., 2004; Ferguson et al., 2001; James and Rushton, 2002; Grubman and Baxt, 2004).

Conventional control measures of FMD include movement restriction (e.g. through construction of 'veterinary boundaries', i.e.

* Corresponding author. Tel.: +1 5197600925.
E-mail addresses: rnotice@uoguelph.ca, noticeringa@yahoo.com (N. Ringa).

http://dx.doi.org/10.1016/j.epidem.2014.09.008

cordon fences erected to divide a country into multiple subregions to prevent movement of animals across the borders); public education; quarantine; vaccination and culling (Barteling, 2002). Control measures of FMD need to take into account the natural characteristics of the virus, mechanism of spread, as well as strategic implementation based on available resources (Cruz-Aponte et al., 2011; Roy et al., 2011). Because of their greater resources, most developed countries have managed to contain, eradicate and avoid importation of FMD virus into their territories. However the disease is still an impediment to more than 100 developing and transitional countries (Bruckner and Saraiva-Vieira, 2010; Kobayashi et al., 2007; Rweyemamu, 2002; Patterson, 2001), mostly in South America, Africa and the Middle East (Kitching, 1998). The types of animals affected by FMD have long been a source of food, transportation, medicine, entertainment, clothing, and financial security for humans (Evans, 2006). Hence, the impact of FMD can extend beyond economics in many developing and transitional countries, where possession of domestic animals such as cattle in many cultural or religious groups is still seen as a symbol of wealth and high social status (Evans, 2006).

The rich database for the dynamics and control of the 2001 FMD outbreak in the United Kingdom (UK) has, of recent, inspired many researchers to develop and analyze mathematical models of the disease (Tildesley et al., 2006), with an intention to inform policy (Garnett, 2002) on better disease control strategies. This had led to many studies focusing on dynamics of a single epidemic outbreak (characteristic of developed countries where FMD outbreaks are rare). Two basic forms of vaccination usually considered are prophylactic vaccination (pre-outbreak vaccination of farms in an at-risk population to prevent introduction of the disease) and ring vaccination (carried out during outbreaks on farms deemed to be at risk of infection due to their geographical proximity to infectious farms (Keeling et al., 2003).

Methods of culling considered by most models include infected premises (IP) culling (slaughtering infected farms), dangerous contacts (DC) culling (culling in premises where animals may have been in direct or indirect contact with infected animals) and contagious premises (CP) culling (slaughtering of farms that border infected premises) (Keeling et al., 2003; Tildesley et al., 2009; Parham et al., 2008). However, few mathematical models of FMD have investigated impacts of constrained vaccination and culling in 'near-endemic' settings, where FMD outbreaks occur repeatedly due to re-introductions from nearby wild endemic populations.

Tildesley et al. (2006) develop a probabilistic transmission model of FMD and explore an optimal deployment strategy of limited reactive ring vaccination of cattle in a single epidemic outbreak. Neilan and Lenhart (2010) construct and numerically analyze single-outbreak, deterministic, mean-field equations (they assume homogeneous mixing of host population) based on an SEIR (susceptible, exposed, infected, recovered) natural history of FMD to illustrate impacts of constrained vaccine supply on optimal vaccination schedule. Rico-Ramirez et al. (2010) apply stochastic optimal control theory, and incorporate spatiality, to study impacts of constrained vaccination supply on an epidemic outbreak of FMD. Hansen and Day (2011) construct a compartmental SIR (susceptible,infectious, recovered) model that explores impacts of limited isolation resources and limited vaccination resources. This approach is also tailored to FMD-free settings. While they appreciate the benefits of investigating impacts of constrained vaccination, Porphyre et al. (2013) focus on benefits of vaccination given triggers such as change in location of epidemic outbreak, and delay in implementation of vaccination and develop a spatial premises based model using data from FMD situation in Scotland. Ferguson et al. (2001) analyze data from the FMD epidemic outbreak in the United Kingdom in 2001 and parameterize a pair approximation model to capture spatial spread, and predict future outbreaks and potential impacts of vaccination (vaccination was not used during the UK 2001 FMD epidemic outbreak). Parham et al. (2008) also develop and study a pair approximation model of FMD which describes dynamics and control (by culling) of a single outbreak. They further present the derivation of a spatially oriented expression of the basic reproduction number (the expected number of secondary cases produced by a single infection in a completely susceptible population (Bauch, 2005; Parham et al., 2008; Brauer, 2006)), from which impacts of culling can be measured.

The following description of pair approximation (PA) models is adapted from Ringa and Bauch (2014), Bauch (2005), Keeling et al. (1997), Parham et al. (2008). PA models are regarded to as the simplest extension of the mean field equations because while the latter are formulated under an assumption that members of the host population of farms mix homogeneously, such that an infectious farm can transmit the virus to any susceptible farm in the population, the former implicitly incorporate spatiality by modeling pairs of neighbouring farms, and assume that events such as infection can take place only between connected farms. In the context of FMD, connection between farms can be described in terms geographical distance or other forms of interaction like business ties which may enhance transmission of the virus. A PA model comprises of a system of ordinary differential equations called pair equations. The derivation of an equation of motion for a pair of farms will involve triples; equations of motion for triples will involve quadruples, etc. To obtain a manageable system of equations of motion we truncate this hierarchy by a technique called moment closure approximations (MCA). There exist several MCAs at the level of pairs (also known as pair approximations), but all of them are used to approximate the resulting triples in terms of lower order correlations, i.e. pairs and singletons. MCAs differ in their assumption of the distribution of farms in a network. The choice of a MCA depends on the intent of the studies or characteristics of the disease spread. For instance, for a triple involving nodes X, Y and Z the ordinary pair approximation (OPA) assumes conditional independence of disease statuses of farms such that a farm X is related to a farm Z, only because they are both directly connected to Y, i.e. no triangles. Another widely used MCA at the level of pairs is the triangular pair approximation (TPA). The distinguishing feature between the OPA and the TPA is that the latter allows for the existence of triangles in the population of farms.

Here we develop an SEIRVC (susceptible, exposed, infectious, recovered, vaccinated, culled) pair approximation model of FMD transmission in a near-endemic population, and explore the impact of constrained vaccination and culling on long-term dynamics of the disease. The model is intended to apply to resource-limited countries subject to repeated disease re-introductions, such as Botswana. In Botswana, farms are dominated by cattle, seasonal movement of farm animals due to nomadism is minimal, veterinary boundaries are widely used, both vaccination and culling are applied (although only culling is applied in certain regions), and farming regions experience repeated re-introductions from neighbouring wild populations where FMD is endemic. The longer time horizon that repeated outbreaks and frequent disease re-introduction impose on disease control, and the wider use of vaccination in such countries, makes factors such as waning vaccine and natural immunity important (Ringa and Bauch, 2014). Our objective is to illustrate features of FMD dynamics and control through vaccination and culling that are unique to resource-limited, near-endemic settings, in contrast to the broad literature on FMD modelling in higher-income, disease-free settings. Both the rates of culling and possible number of culls per epidemic outbreak may be dependent on the availability of resources such as manpower, equipment for culling and disposal of carcasses. Vaccine supplies are likewise limited by the stockpile available, and so authorities face a decision regarding when and how to vaccinate

farms. As outcome measures, we explore both the final size of outbreaks, as well as social impacts. Social impact is defined by total animals culled or infected, and is intended to reflect the broader social significance of animals in some low-income countries (Evans, 2006). The model structure is described in the following section.

2. Model description

We build on a previous pair approximation model of FMD (Ringa and Bauch, 2014). Cattle are highly susceptible to FMD and this enables the virus to spread rapidly to the entire herd (Depa et al., 2012; Grubman and Baxt, 2004). Thus it is difficult to track down the spread of FMD from one animal to another within a farm. Hence, the farm is taken as the fundamental epidemiological unit in our model, in line with a common assumption in the literature on pair approximation FMD models (Ringa and Bauch, 2014; Parham et al., 2008; Ferguson et al., 2001).

The state variables of our model are singletons, $[X]$ and pairs, $[XY]$, representing the number of farms whose disease status is X, and the number of neighbouring pairs of farms comprising of status X and status Y farms, respectively. Transmission at a rate τ takes place between an infectious and a neighbouring susceptible farm, moving the latter to the exposed compartment. The population of farms is assumed to exist on a random contact network with Poisson-distributed neighbourhood size. However, the network is conceived to represent an underlying spatial point-process model with an infection kernel. Bauch and Galvani (2003) show that a properly parameterized network model can approximate epidemic dynamics of a spatial point-process model with an infection kernel, for parameters such that the infection is endemic in the absence of interventions. We also carried out the full analysis for a scenario where farms are distributed on a regular lattice, and we found that this did not qualitatively change the results.

A farm stays in the exposed state for ν^{-1} days on average (latent period), after which it becomes infectious. The recovery rate is σ. The natural immunity waning rate is ω, enabling transition of farms from R to S compartments. Prophylactic vaccination and ring vaccination occur at per capita rates ψ_p and ψ_r, respectively, and transfer vaccinated susceptible and exposed farms to the vaccinated compartment. The rate of loss of vaccine-induced immunity (vaccine waning) is θ (where farms lose protection from the vaccine, becoming susceptible again). We explore IP culling and DC culling (defined as slaughtering of non-infectious farms neighbouring an infected farm on the contact network) Whenever a DC cull occurs, the infected farm that prompted the cull is also culled (IP culling), but we refer to both processes inclusively as 'DC culling' throughout, for simplicity. The rates of IP and DC culling are μ_{IP} and μ_{DC}, respectively, and previously culled farms are replaced (joining the susceptible pool) at a rate η. Because links in a contact network can be taken to represent any kind of potentially effective contact between farms and because we do not model space explicitly, we interpret culling of a network neighbour as DC culling rather than CP culling, which is implemented in a geographically spatial environment.

The rates of transition between compartments are expressed mathematically so that the model is formulated as a system of ordinary differential equations. In Appendix A we illustrate the derivation of the equation of motion for $[SI]$ and present the full pair approximation model. Two forms of the ordinary pair approximation (OPA) are usually used: the binomial OPA (applicable to regular networks where the number of contacts per farm is fixed) and the Poisson OPA (applies in random networks where the neighbourhood size varies from one individual farm to another). In this paper we approximate triples by the Poisson OPA, see Eq. (A.3).

2.1. The basic reproduction number

The analytical tractability of pair approximation models enables the derivation and analysis of epidemiologically important features such as the basic reproduction number, R_0, defined as the expected number of secondary cases produced by a single infection in a completely susceptible population (Bauch, 2005; Parham et al., 2008; Brauer, 2006). An epidemic is possible if $R_0 > 1$ but the infection will die out if $R_0 < 1$. Our expression of the basic reproduction number captures spatiality by virtue of the fact that its derivation uses the correlation function, C_{XY} between farms with disease statuses X and Y:

$$C_{XY} = \frac{N}{n}\frac{[XY]}{[X][Y]}, \tag{1}$$

where n is the average number of neighbours per farm and N is the total population size (Keeling et al., 1997; Parham et al., 2008). $C_{XY} = 1$ corresponds to mass-action mixing; $C_{XY} > 1$ aggregation and $C_{XY} < 1$ avoidance of farm types X and Y. It is worth noting that under mean-field approximations where $n = N$ (because it is assumed that all susceptible individuals farms are equally likely to acquire the disease from any infectious farm in the population) and $[XY] = [X][Y]$, correlation between two farms remains constant at $C_{XY} = 1$, through time. However under pair approximations, it is possible to derive an expression for R_0 by taking advantage of biological intuition about the geometric structure of early invading clusters of infected farms. In particular, infected farms tend to cluster together on the network in the early stages of invasion, which has implications for the efficiency of disease transmission and hence the R_0. Such effects enable us to relate correlations between susceptible and infectious farms (C_{SI}) to correlations between exposed and infectious farms (C_{EI}) (Bauch, 2005; Parham et al., 2008). A more detailed description is provided in Appendix B and the resulting expression for R_0 is

$$R_0 = \frac{\tau n C_{SI}^*}{(\psi_r + \mu_{DC})n(([E]/N)C_{EI})^* + (\sigma + \mu_{IP})}. \tag{2}$$

C_{SI}^* and $(([E]/N)C_{EI})^*$ are defined explicitly in Appendix B.

At first glance, Eq. (2) reveals that a high recovery rate σ, corresponds to a low value of the basic reproduction number. This is because increasing σ leads to a significant decrease of the number of infectious farms (therefore reducing the spread). Also from Eq. (2) it is apparent that the transmission rate τ, increases the basic reproduction number while vaccination and culling reduce R_0. We point out, however, that the actual impacts of model parameters, including rates of control measures, can be modeled numerically using the full expression of the basic reproduction number presented in Appendix B.

2.2. Baseline parameters

After contact with the virus, it takes between 2 and 14 days for cattle, swine, sheep, goats and deers to show symptoms of FMD (Mushayabasa et al., 2011). According to Mardones et al. (2010) the latent period of FMD is 3.1–4.8 days in cattle. Keeling et al. (2001) claims this period is 4–5 days. Here we average over these values and assume that the latent period of FMD in cattle is 4 days, thus $\nu = 1/4 = 0.25$ day^{-1}. Depending on animal species affected, infected animals remain symptomatic of FMD and infectious for about 7–10 days before they recover, (Grubman and Baxt, 2004). Here we assume that the recovery rate is $\sigma = 1/7 = 0.143$ day^{-1}. Farms in Botswana tend to be dominated by cattle, hence our natural history parameter values are those specific to cattle.

The length of natural and vaccine protection from FMD ranges from 6 months to 5.5 years, depending on species affected, the virus serotype, and type of vaccine administered (Doel, 1996;

Keeling et al., 2003). Our baseline choices of rates of natural immunity waning and vaccine waning are $\omega = 1/180 = 0.0056$ day^{-1} and $\theta = 1/180 = 0.0056$ day^{-1}, respectively. We fix the population size at $N = 40,000$ farms and assume that per capita vaccination rates of prophylactic and ring vaccination, ψ_p and ψ_r, take values between 0 day^{-1} and 0.006 day^{-1}. The predicted vaccination capacity in a higher-income country such as Scotland has been approximated as 136 farms per day (Porphyre et al., 2013). For an absolute upper limit on ψ_p and ψ_r we choose 0.006 day^{-1}, which corresponds to vaccinating 240 farms per day in a population of 40,000 farms. We chose a relatively generous upper bound for the vaccination rate to illustrate what could be accomplished in resource-limited settings, if greater resources were eventually made available.

During the 7 month-long FMD outbreak in Great Britain in 2001, over 11,000 farms were culled (Tildesley et al., 2009). This corresponds to 50 farms per day on average, although the rate was much higher during the peak of the epidemic. We assume that rates of IP culling, μ_{IP} and DC culling, μ_{DC}, take values between 0 day^{-1} and 0.25 day^{-1}. For a prevalence of 2.5 % in a population of 40,000 farms, this corresponds to an upper bound of 250 farms culled per day. As with vaccination, we chose a relatively generous upper bound to the culling capacities to illustrate what could be possible in resource-limited settings, if greater resources were eventually devoted to FMD control.

We also assume that farmers are compensated for culled farms at a rate $\eta = 1/1464 = 0.00068$ day^{-1} (i.e. compensation is carried out after 4 years, which reflects the situation in near-endemic, resource-limited settings).

Our baseline value for the transmission rate is taken from a similar model in Ringa and Bauch (2014), where $\tau = 0.6$ day^{-1} was derived from the basic reproduction number. This value also yields epidemiologically plausible responses to realistic intervention levels (Ringa and Bauch, 2014). However, we also explore scenarios with $\tau = 0.3$ day^{-1} (corresponding to a large average distance or low level of interaction between infectious and susceptible farms), and $\tau = 0.9$ day^{-1} (corresponding to a small average distance or high level of interaction between infectious and susceptible farms) in sensitivity analysis. Changes in the value of τ implicitly capture both changes in the spatial location of farms, with higher values corresponding to higher farm density, as well as any changes in average herd size or herd composition, though not between-farm heterogeneities.

In some countries, foot and mouth disease can spread across borders through animal movement or trade. In some parts of Botswana FMD is imported from Zimbabwe or South Africa resulting in a series of outbreaks almost every 2 years (Mokopasetso and Derah, 2005). Model simulations in our study are run under a presumption that the disease is re-introduced into the population of farms every 800 days (just over 2 years). We summarize all baseline parameters in Table 1.

Table 1
Baseline parameters for our model.

Parameter	Value	Source
Transmission, τ	0.6 day^{-1}	Ringa and Bauch (2014)
Latency, ν	0.25 day^{-1}	Mardones et al. (2010), Mushayabasa et al. (2011), Keeling et al. (2001)
Recovery, σ	0.143 day^{-1}	Parham et al. (2008)
Natural immunity waning, ω	0.0056 day^{-1}	Doel (1996)
Ring vaccination, ψ_r	(0–0.006) day^{-1}	Calibrated
Prophylactic vaccination, ψ_p	(0–0.006) day^{-1}	Calibrated
Vaccine waning, θ	0.0056 day^{-1}	Doel (1996), Keeling et al. (2003)
IP culling, μ_{IP}	(0–0.25) day^{-1}	Calibrated
DC culling, μ_{DC}	(0–0.25) day^{-1}	Calibrated
Replacement of culled farms, η	0.00068 day^{-1}	Assumption

2.3. Constraints of vaccination and culling capacity

Let $X_p(t)$ and $X_r(t)$ be the cumulative number of farms prophylactically vaccinated and ring vaccinated since the beginning of the year, respectively, at any given time t. We define the 'vaccine capacity' as the total number of farms that can be vaccinated in a given year. Let V_i, $i = 1, 2, 3\ldots$, be the vaccine capacity in a given year. Let ψ_p and ψ_r be the rates of prophylactic vaccination and ring vaccination, respectively. Also, let $\psi_p^{\max}, \psi_r^{\max} \in [0, 0.0060]^2$ describe maximal possible rates of prophylactic and ring vaccination. For each year, $\psi_p = \psi_p^{\max}$, $\psi_r = \psi_r^{\max}$ as long as $X_p + X_r \leq V_i$. However, as soon as the vaccine capacity V_i is reached, $\psi_p = \psi_r = 0$ day^{-1} for the remainder of the year. That is, each year, vaccination is deployed until maximum vaccine supply is reached, after which the outbreak progresses without additional control measures. At the beginning of the following year, $\psi_p = \psi_p^{\max}$, $\psi_r = \psi_r^{\max}$ and the process repeats. We assume that the vaccine is 100 % effective at the farm level and all vaccinated farms are protected from infection for the duration of vaccine immunity, although in reality the effectiveness at the level of the individual animal can be less than 100 %, due to strain mismatch for example.

Culling rates can also be constrained. If C_i, $i = 1, 2, 3, \ldots$, is the maximum possible culling rate in a year, determined by available manpower, then corresponding rates of IP culling, $\mu_{IP}^{\max}$, and DC culling, $\mu_{DC}^{\max}$, depend on C_i and the network structure such that $(n+1)\mu_{IP}^{\max} + \mu_{DC}^{\max} = C_i$, where n is the average number of neighbours each farm has and $\mu_{IP}^{\max}, \mu_{DC}^{\max} \in [0, 0.25]^2$. This equation incorporates the idea that DC culling of farms neighbouring an infected premises, implies that the infected farm is also culled.

Finally, we also explore scenarios where the total number of culled farms is constrained. Let $Y_{IP}(t)$ and $Y_{DC}(t)$ be the cumulative number of farms IP-culled and DC-culled since the beginning of the year, respectively, at any given time and let Y_i, $i = 1, 2, 3\ldots$ be the possible number of culled farms in a given year. Let $\mu_{IP}^{\max}, \mu_{DC}^{\max} \in [0, 0.25]^2$ describe the corresponding maximal possible rates of IP and DC culling. For each each year, if $Y_{IP} + Y_{DC} \leq Y_i$, then $\mu_{IP} = \mu_{IP}^{\max}$, $\mu_{DC} = \mu_{DC}^{\max}$, but once once Y_i is reached, then $\mu_{IP} = \mu_{DC} = 0$ day^{-1} for the remainder of the year.

3. Results and discussion

We first explore the impacts of constrained vaccination in the absence of culling. The total number of vaccines administered is constrained according to the equation $X_p + X_r \leq V_i$. For any given rates of prophylactic vaccination $\psi_p^{\max}$, and ring vaccination $\psi_r^{\max}$, increasing the vaccine capacity, V_i, always brings about more vaccine coverage, leading to a decrease in cumulative infections over a 20 year period (Fig. 1). Hence, as expected, increasing vaccine capacity is desirable whenever possible. However, if it is not possible to increase vaccine capacity, then a decision-maker faces the choice of how to optimize the rates of vaccination $\psi_p^{\max}$ and $\psi_r^{\max}$. When vaccine capacity is relatively low (e.g. Fig. 1a), the highest rates of prophylactic vaccination $\psi_p^{\max}$ actually produce more cumulative infections than intermediate rates falling within the darker regions of Fig. 1a ($\psi_r^{\max} = 0.0060$ day^{-1}). The optimal ring vaccination rate remains at approximately $\psi_r^{\max} = 0.0060$ day^{-1} (the maximum possible value in the range of values considered) while the optimal prophylactic vaccination rate increases gradually from $\psi_p^{\max} = 0.0005$ day^{-1} (Fig. 1a) to $\psi_p^{\max} = 0.0022$

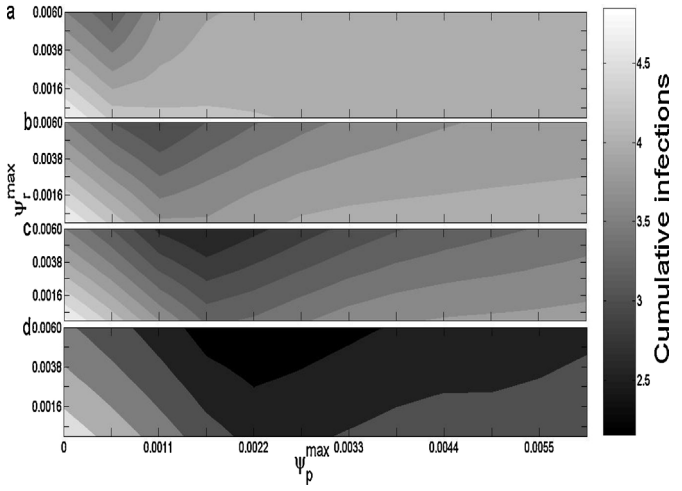

Fig. 1. Cumulative infections in 20 years versus rates of prophylactic vaccination, ψ_p^{max}, and ring vaccination, ψ_r^{max}, for vaccine capacities $V_i = 6000$ per year (a), $V_i = 10000$ per year (b), $V_i = 14000$ per year (c) and $V_i = 18000$ per year (d). Model parameters are in Table 1.

day^{-1} (Fig. 1d) as V_i increases from 6000 per year to 18,000 per year. At higher values of ψ_p^{max}, the supply of vaccine is used up before the year is finished, while at the lower, more optimal values of ψ_p^{max}, it lasts throughout the year. This observation implies that optimally controlling FMD when vaccine capacity is strongly constrained requires spreading out available supplies for prophylactic vaccination over the course of the year, while during outbreaks, ring vaccination should always be deployed as rapidly as possible.

Table 2 summarizes the optimal rates of prophylactic and ring vaccination for a range of values of vaccine capacity V_i. These results assume the baseline transmission rate $\tau = 0.6$ day^{-1}. Decreasing the transmission rate ($\tau = 0.3$ day^{-1}) decreases the overall number of cumulative infections, while increasing the transmission parameter ($\tau = 0.9$ day^{-1}) yields more cumulative infections (Online supplementary material Fig. S1). However, in agreement with the observation made from Fig. 1, the conclusion that when vaccination capacity is strongly constrained, the optimal ring vaccination rate remains constant at the maximum possible value in the range of values considered, while the optimal prophylactic vaccination rate increases gradually from low to higher values as V_i increases, also holds for lower or higher values of τ (Online supplementary material Fig. S1).

In agreement with Fig. 1, the rate of prophylactic vaccination that yields minimum cumulative infections remains well below the maximum permissible value across a wide range of values of V_i, although the optimal value increases gradually with increasing V_i, up to a value of $\psi_p^{max} = 0.0033$ day^{-1} for $V_i = 24,000$ (Table 2). In contrast, the optimal rate of ring vaccination remains constant at the maximal value $\psi_r^{max} = 0.0060$ day^{-1}. The total number of vaccines administered through ring vaccination is relatively small compared to the total number of vaccines administered prophylatically, since ring vaccination at a sufficiently high rate is sufficient to end an outbreak quickly, resulting in a relatively small number of ring-vaccinated farms (Table 2). Results are qualitatively similar for lower and higher transmission rates τ (Online supplementary material, Tables 3 and 4).

Time series of the number of infectious farms and number of vaccinated farms for various rates ψ_p^{max} show why it is better to spread out prophylactic vaccination over the course of the year (Fig. 2). These time series illustrate to the third row of Table 2. We observe that when $\tau = 0.6$ day^{-1} then for $V_i = 10,000$ vaccines per year, the optimal rate of prophylactic vaccination $\psi_p^{max} = 0.0011$ day^{-1}

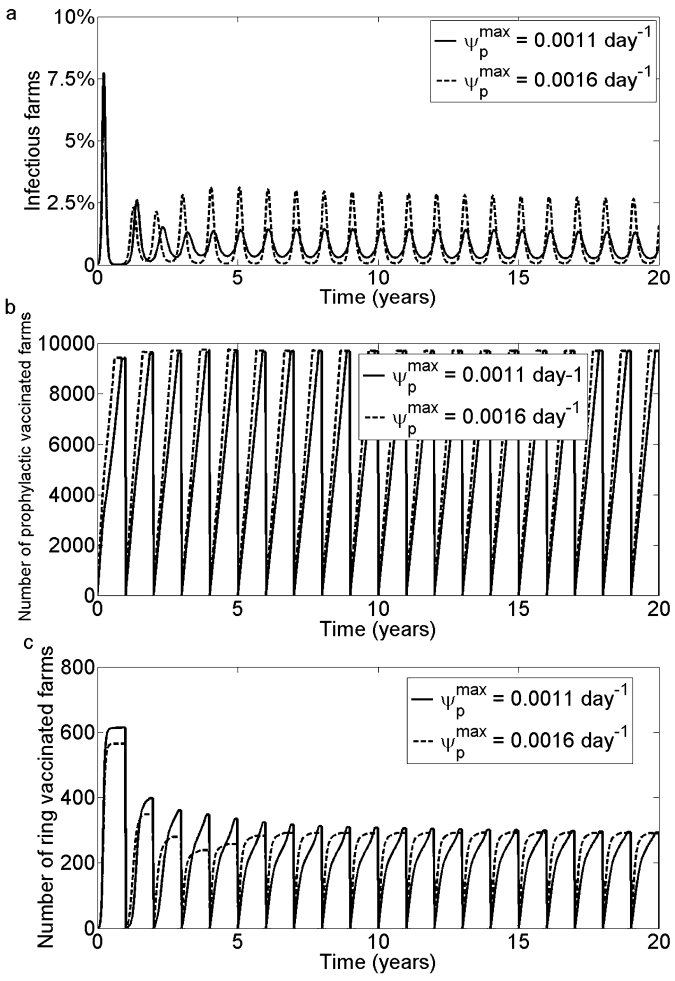

Fig. 2. Time series for number of infectious farms (a), number of prophylactic vaccinated farms (b) and number of ring vaccinated farms (c) varying rates of prophylactic vaccination, ψ_p^{max}. $V_i = 10000$ per year, $\psi_r = 0.0060$ day^{-1} and parameters are in Table 1.

prevents larger outbreaks, and the percentage of infectious farms remains below 1.5% (Fig. 2a) and the vaccine supply lasts for most of the year (Fig. 2b). However, at a higher rate $\psi_p^{max} = 0.0016$ day^{-1}, the vaccine supply runs out much earlier in the year (Fig. 2b). Every few years, this event is followed a few months later by large peaks in infection prevalence, surpassing 3%, and occurring before the supply is renewed the following year (Fig. 2a).

We point out that waning of vaccine immunity plays a large role here. If vaccine immunity did not wane so quickly, a strategy of vaccinating at rate $\psi_p^{max} = 0.0016$ day^{-1} might work better, since vaccine protection would extend for a longer time, after the vaccine supply ran out. This is confirmed by sensitivity analysis (Online supplementary material, Table 5). Thus the optimal rates of prophylactic and ring vaccination depend on the duration of natural immunity and vaccine immunity, such that when these durations are increased (i.e reduction of rates of natural immunity waning, ω and vaccine waning, θ), higher rates of prophylactic vaccination are optimal.

A decrease in the rate of disease importation causes a decrease in cumulative infections (Online supplementary material, Fig. S2). This signifies the importance of putting measures in place to avoid disease re-introduction, for instance by managing animal movement and erecting cordon fences around farms. It also illustrates how cumulative infections can be determined by nonlinear interactions between vaccine capacity and disease re-introduction

Table 2
Minimum cumulative infections in 20 years, corresponding optimal rates of prophylactic vaccination, $\psi_p^{\max}$, and ring vaccination, $\psi_r^{\max}$, varying vaccine capacities, V_i, and yearly average number of prophylactic and ring vaccines used. Model parameters are in Table 1.

V_i	Min. cum. infec	$\psi_p^{\max}$	$\psi_r^{\max}$	Avg. yearly proph.	Avg. yearly ring
6000	32,3160	0.0005 day^{-1}	0.0060 day^{-1}	5599	401
8000	31,3059	0.0011 day^{-1}	0.0060 day^{-1}	7648	352
10,000	29,6160	0.0011 day^{-1}	0.0060 day^{-1}	9675	325
12,000	28,6434	0.0016 day^{-1}	0.0060 day^{-1}	11,693	307
14,000	25,8370	0.0016 day^{-1}	0.0060 day^{-1}	13,711	289
16,000	24,4865	0.0022 day^{-1}	0.0060 day^{-1}	15,761	239
18,000	21,5640	0.0022 day^{-1}	0.0060 day^{-1}	17,782	218
20,000	18,8626	0.0027 day^{-1}	0.0060 day^{-1}	19,799	201
22,000	16,7850	0.0027 day^{-1}	0.0060 day^{-1}	21,814	186
24,000	14,5680	0.0033 day^{-1}	0.0060 day^{-1}	23,831	169

Table 3
Minimum cumulative infections in 20 years, corresponding optimal rates of prophylactic vaccination, $\psi_p^{\max}$, and ring vaccination, $\psi_r^{\max}$, varying vaccine capacities, V_i, and yearly average number of prophylactic and ring vaccines used. $\tau = 0.3$ day^{-1} and other parameters are in Table 1.

V_i	Min. cum. infec	$\psi_p^{\max}$	$\psi_r^{\max}$	Avg. yearly proph.	Avg. yearly ring
6000	18,5080	0.0005 day^{-1}	0.0060 day^{-1}	5664	336
8000	178,148	0.00075 day^{-1}	0.0060 day^{-1}	7765	235
10,000	152,640	0.0011 day^{-1}	0.0060 day^{-1}	9770	230
12,000	138,290	0.0011 day^{-1}	0.0060 day^{-1}	11,808	192
14,000	111,110	0.0016 day^{-1}	0.0060 day^{-1}	13,829	171
16,000	83,303	0.0016 day^{-1}	0.0060 day^{-1}	15,848	152
18,000	58,175	0.0016 day^{-1}	0.0060 day^{-1}	17,902	98
20,000	36,631	0.0022 day^{-1}	0.0060 day^{-1}	19,921	79
22,000	12,870	0.0022 day^{-1}	0.0060 day^{-1}	21,952	48
24,000	6168	0.0027 day^{-1}	0.0060 day^{-1}	23,963	37

rates, suggesting that vaccine programs and movement restrictions should be designed in an integrated way in near-endemic settings.

Next, we manipulated culling rates in the absence of vaccination, where culling rates ($\mu_{IP} = \mu_{IP}^{\max}$ and $\mu_{DC} = \mu_{DC}^{\max}$) are constrained by the equation $(n+1)\mu_{IP}^{\max} + \mu_{DC}^{\max} = C_i$, where $\mu_{IP}^{\max}, \mu_{DC}^{\max} \in [0, 0.25]^2$ and n is the average neighbourhood size. (We remind the reader that, whenever a DC cull occurs, the infected premises that simulated the DC cull is also culled.) As expected, increasing the culling rate capacity, C_i reduces cumulative infections and size of epidemic peaks (Fig. 3).

However, the size of this reduction depends on the culling capacity. When the culling rate capacity C_i is small, the cumulative number of infections is smallest when μ_{DC} is large. For instance, when $C_i = 0.6$, then the cumulative number of infections is smallest when the rate of DC culling is $\mu_{DC}^{\max} = 0.25$ day^{-1} (Fig. 3a; we note that the corresponding rate of IP culling at this point is $\mu_{IP}^{\max} = 0.07$ day^{-1}). However, when the culling capacity is large, the

Table 4
Minimum cumulative infections in 20 years, corresponding optimal rates of prophylactic vaccination, $\psi_p^{\max}$, and ring vaccination, $\psi_r^{\max}$, varying vaccine capacities, V_i, and yearly average number of prophylactic and ring vaccines used. $\tau = 0.9$ day^{-1} and other parameters are in Table 1.

V_i	Min. cum. infec	$\psi_p^{\max}$	$\psi_r^{\max}$	Avg. yearly proph.	Avg. yearly ring
6000	375,630	0.0005 day^{-1}	0.0060 day^{-1}	5447	553
8000	359,990	0.00075 day^{-1}	0.0060 day^{-1}	7622	378
10,000	350,150	0.0011 day^{-1}	0.0060 day^{-1}	9694	306
12,000	333,240	0.0011 day^{-1}	0.0060 day^{-1}	11,704	296
14,000	313,920	0.0016 day^{-1}	0.0060 day^{-1}	13,726	274
16,000	301,210	0.0022 day^{-1}	0.0060 day^{-1}	15,739	261
18,000	271,060	0.0022 day^{-1}	0.0060 day^{-1}	17,741	259
20,000	252,700	0.0027 day^{-1}	0.0060 day^{-1}	19,756	244
22,000	224,090	0.0027 day^{-1}	0.0060 day^{-1}	21,774	226
24,000	202,960	0.0033 day^{-1}	0.0060 day^{-1}	23,789	211

Table 5
Minimum cumulative infections in 20 years, corresponding optimal rates of prophylactic vaccination, $\psi_p^{\max}$, and ring vaccination, $\psi_r^{\max}$, varying vaccine capacities, V_i, and yearly average number of prophylactic and ring vaccines used. $\omega = \theta = 1/270$ day^{-1} and other parameters are in Table 1.

V_i	Min. cum. infec	$\psi_p^{\max}$	$\psi_r^{\max}$	Avg. yearly proph.	Avg. yearly ring
6000	202,750	0.00075 day^{-1}	0.0060 day^{-1}	5771	229
8000	181,049	0.0011 day^{-1}	0.0060 day^{-1}	7802	198
10,000	159,040	0.0016 day^{-1}	0.0060 day^{-1}	9821	179
12,000	137,902	0.0016 day^{-1}	0.0060 day^{-1}	11,841	159
14,000	110,740	0.0022 day^{-1}	0.0060 day^{-1}	13,868	132
16,000	87,843	0.0022 day^{-1}	0.0060 day^{-1}	15,898	102
18,000	59,802	0.0027 day^{-1}	0.0060 day^{-1}	17,909	91
20,000	33,367	0.0033 day^{-1}	0.0060 day^{-1}	19,946	54
22,000	17,661	0.0055 day^{-1}	0.0060 day^{-1}	21,977	23
24,000	14,568	0.0055 day^{-1}	0.0060 day^{-1}	23,991	9

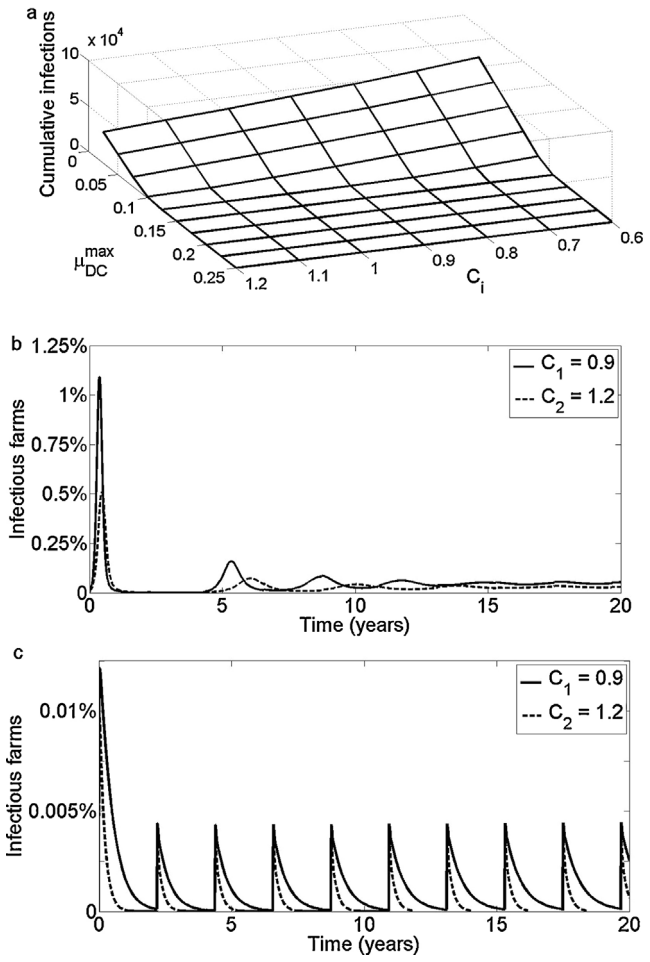

Fig. 3. Cumulative number of infectious farms in 20 years as a function of **DC** culling, $\mu_{DC}^{\max}$ (and IP culling, $\mu_{IP}^{\max}$), and culling rate capacity, C_i (a). Time series for infectious farms where $\mu_{DC}^{\max} = 0.025$ day^{-1} (b) and $\mu_{DC}^{\max} = 0.125$ day^{-1} (c). $n = 4$ and other parameters are in Table 1.

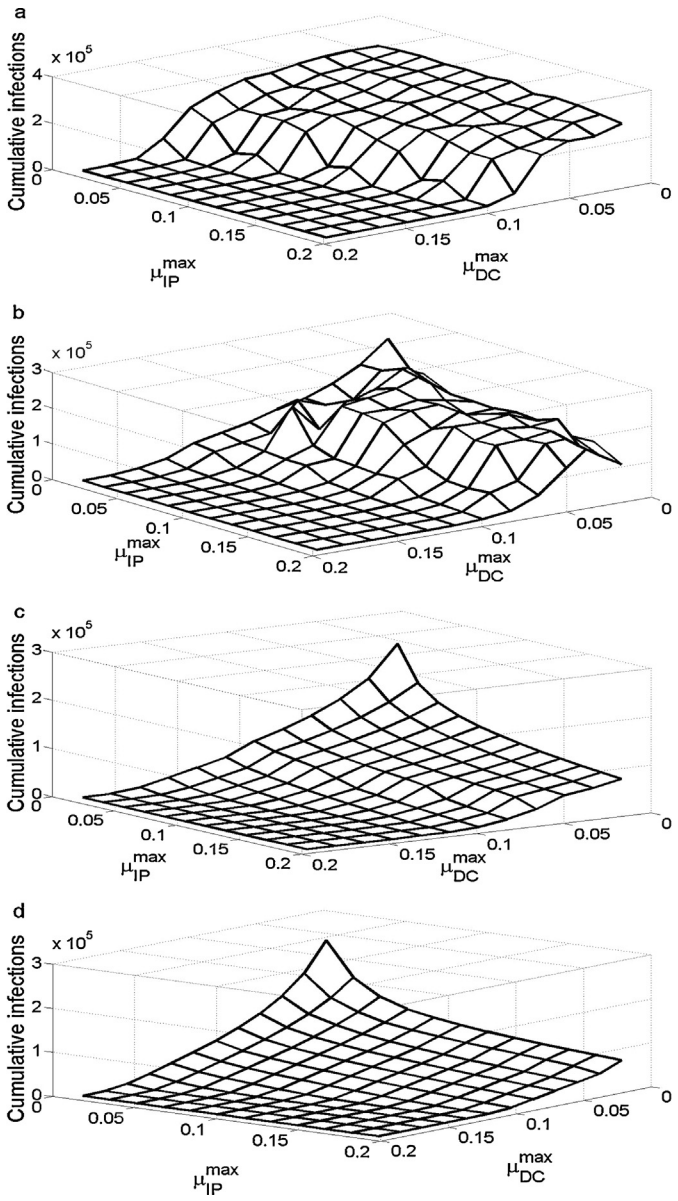

Fig. 4. Cumulative number of infectious farms in 20 years as a function of IP culling, $\mu_{IP}^{\max}$ and **DC** culling, $\mu_{DC}^{\max}$ where upper boundaries of the number of culled farms are $Y_i = 1000$ per year (a), $Y_i = 2000$ per year (b), $Y_i = 4000$ per year (c) and $Y_i = 8000$ per year (d). Model parameters are in Table 1.

cumulative number of infections is relatively small regardless of the value of $\mu_{DC}^{\max}$ (Fig. 3a). This implies that when culling capacity is small, it is better to concentrate resources into DC culling. However, if culling capacity is sufficiently large, then either IP or DC culling may be used, if their rates are high enough. The impact of changes in C_i is clear when culling rates are low (Fig. 3b), but less apparent when culling rates are large, and the disease is essentially eradicated (Fig. 3c: here rates of culling are so large that re-introduction of the disease every 800 days fails to set off an epidemic outbreak).

We also explored the impact of limiting the total number of culls allowed per year Y_i (described in Section 2.3). Increasing Y_i, decreases the number of cumulative infections (Fig. 4).

We find that in agreement with Fig. 3, when culling capacity Y_i is large, then the number of cumulative infections is relatively small across most possible rates of IP culling, $\mu_{IP}^{\max}$ and DC culling, $\mu_{DC}^{\max}$ and both forms of culling are relatively effective (Fig. 4d). However, when Y_i is small, then the number of cumulative infections is only small when the rate of DC culling, $\mu_{DC}^{\max}$ is sufficiently large, and the results are relatively insensitive to $\mu_{IP}^{\max}$ (Fig. 4a). Hence, when the total number of culls per year must be limited, it is better to put scarce resources into DC culling.

Along the same lines, another observation we can make from Fig. 4 is that DC culling reduces cumulative infections faster than IP culling. For instance in Fig. 4a, the number of cumulative infections decays rapidly with respect to $\mu_{DC}^{\max}$, while the decrease in cumulative infections appears less steep with respect $\mu_{IP}^{\max}$. This holds, but on different scales, even for large values of Y_i. The advantage of DC culling over IP culling is that the former helps get rid of potential new contacts, ensuring that initially infected farms do not have susceptible neighbours to transmit the disease to. In contrast, unless it is applied promptly and rapidly, IP culling alone, may fail to prevent transmission to a neighbouring farm and thus a continued epidemic. The conclusions drawn from Fig. 4 also hold under the high and low transmission rate scenarios ($\tau = 0.3$, 0.9 day^{-1}), except that when the transmission rate is low or when Y_i is large enough then both forms of culling effectively bring the disease under control, and the results are less sensitive to variation of Y_i (Online supplementary material, Fig. S3).

A time series of the number of infectious farms in the situation where the number of farms culled is constrained below $Y_i = 1000$ per year shows how the fewest infections are obtained when culling rates are maximized, which results in rapid containment of the outbreak and thus fewer total culls in the long term (Fig. 5d and a). Confirming the observation established from Fig. 4, when DC

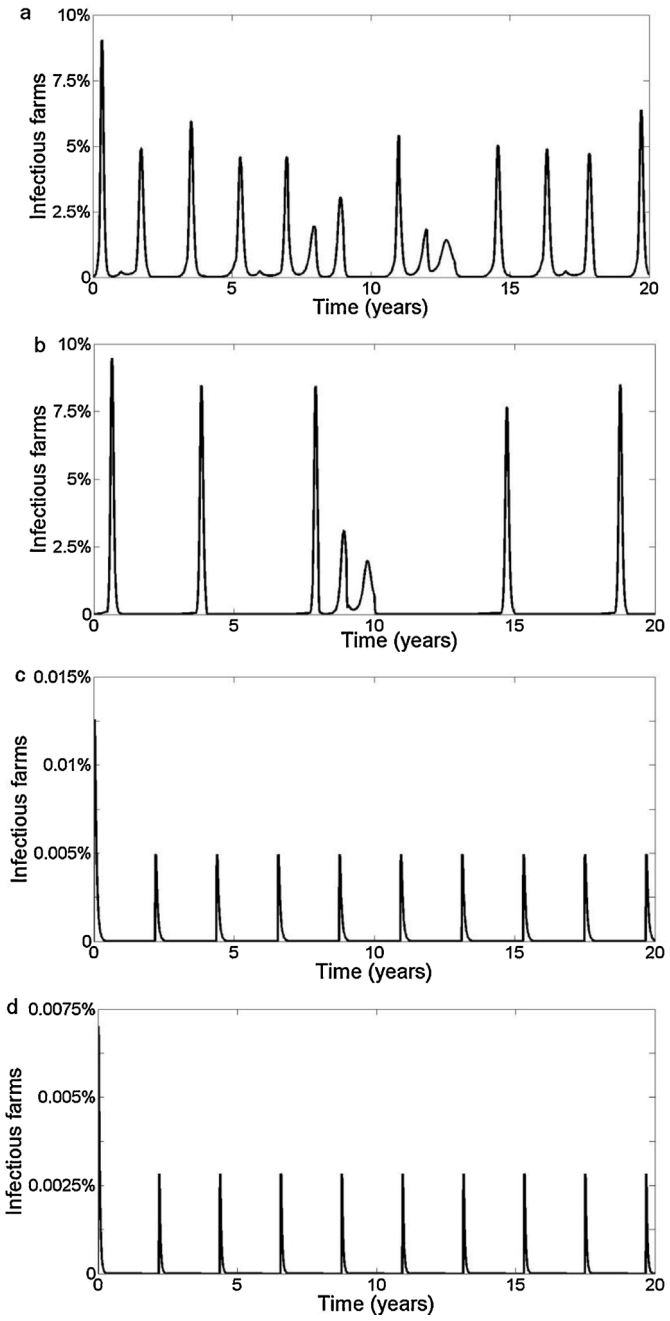

Fig. 5. Time series for number of infectious farms where each year $\mu_{IP}^{max} = \mu_{DC}^{max} = 0.05$ day^{-1} (a), $\mu_{IP}^{max} = 0.25$ day^{-1}, $\mu_{DC}^{max} = 0.05$ day^{-1} (b), $\mu_{IP}^{max} = 0.05$ day^{-1}, $\mu_{DC}^{max} = 0.25$ day^{-1} (c) and $\mu_{IP}^{max} = \mu_{DC}^{max} = 0.25$ day^{-1} (d), before maximum culls, $Y_i = 1000$ per year is reached. Other parameters are in Table 1.

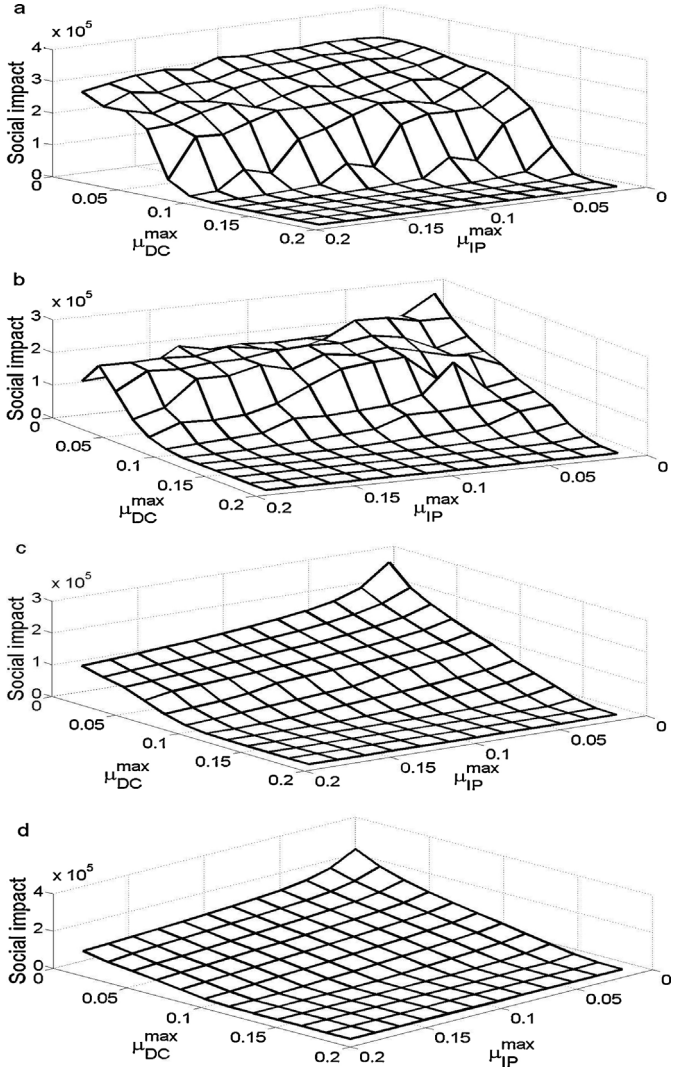

Fig. 6. Social impact in 20 years as a function of IP culling, μ_{IP}^{max} and **DC** culling, μ_{DC}^{max} where upper boundaries of number of culled farms are $Y_i = 1000$ per year (a), $Y_i = 2000$ per year (b), $Y_i = 4000$ per year (c) and $Y_i = 8000$ per year (d). Model parameters are in Table 1.

culling rates are very large, then the constraint $Y_i = 1000$ is never reached (Fig. 5c and d) in contrast to the situation when culling rates are small (Fig. 5a). Also in compliance with previous results, DC culling performs better than IP culling (Fig. 5b and c).

Next, we evaluated the social impact of various control strategies, where social impact was defined as total number of farms infected or culled over a 20 year period. When the total number of annual culls Y_i is constrained, the social impact is smallest when DC culling rates are maximized and this applies across all values of Y_i (Fig. 6). As before, results are less sensitive to changes in the IP culling rate. Hence, social impact at the global, population level is smallest when DC culling is rapidly and vigorously applied at the local level. To permit this strategy to work, identification of infection point source and at-risk farms must be done early during the initial stages of an epidemic outbreak, so that DC culling not only successfully controls the disease but also results in fewer total culled farms, thereby minimizing social impact. While increasing the culling capacity Y_i generally reduces the number of cumulative infections and hence reduces social impact, its impacts are more profound when the transmission rate is large (Online supplementary material, Fig. 4).

In some regions of countries like Botswana, vaccination and culling can be applied simultaneously. Hence, we also explored a scenario where both control measures are applied, under constraints, and compared it to a scenario where only culling is applied. We found that the optimal culling strategy is to maximize the DC culling rate μ_{DC}^{max}, regardless of whether vaccination is also being applied (online supplementary material Fig. S5b and a). Additionally, at lower DC culling rates where culling is not perfectly effective in preventing epidemics, being able to deploy vaccination as well decreases cumulative infections by an order of magnitude, suggesting that the combination of both culling and vaccination is disproportionately more effective than either control measure on its own (online supplementary material Fig. S5b and a).

This model makes necessary simplifications that could influence results. Most notably, we assume that contacts between farms do

not evolve over time, that the per-edge transmission rate and herd size are the same for each farm, and that the average farm density (reflected in average node degree of the Poisson distribution) does not change over the country. In reality, spatial and temporal heterogeneity could impact which control strategies are optimal. Seasonal movements of cattle due to nomadism, as occurs in some lower income countries, could also influence model predictions, although nomadism is not significant in Botswana.

Additionally, high resolution data are generally lacking in low income countries, making it difficult to create the kind of highly realistic country-specific models that were constructed for Great Britain in 2001 for example. However, the impact of heterogeneity on model predictions could be captured to some extent through carefully designed sensitivity analysis. And, even when high resolution data on current farm demographics is available, it is difficult to predict demographic changes over a longer period of time, as required for analyzing endemic or near-endemic situations. However, this is a problem for any model-based evaluation of long-term infectious disease dynamics, such as those undertaken for common endemic infections like measles.

4. Conclusions

Occurrence of repeated FMD epidemics in some developing countries poses a threat to international trade in animals and their products. Lack of resources such skilled manpower, culling resources and vaccine supply, play a vital role in the dynamics and control of FMD in low-income countries with developing economies, as they cause difficulty in eradicating the disease and preventing future outbreaks. Decision-makers in these countries face tighter resource constraints when optimizing their control policies. In this paper we developed a spatially oriented pair approximation model that resembles the dynamics of FMD in some low-income countries subject to near-endemic FMD. We investigated the impacts of constrained vaccination (prophylactic and ring) and culling (IP and DC) capacity on long-term dynamics of FMD.

We conclude that, if vaccine capacity is strongly constrained, then the strategy which minimizes the cumulative number of infections is rapid deployment of ring vaccination during outbreaks. In parallel with ring vaccination (and in contrast to the optimal ring vaccination approach), the rate of prophylactic vaccination must be carefully rationed such that vaccination is stretched out for as long as possible, in order to minimize cumulative long-term infections. This strategy avoids extended periods of time where no prophylactic vaccination is occurring, and during which populations are susceptible to outbreaks. With respect to optimal culling, the best approach is one which involves rapid identification of infected farms and their at-risk neighbours, followed by rapid culling of both infected and at-risk neighbouring premises. In contrast, putting resources into culling only the infected premises is usually less effective, even if more infected premises in total can be culled as a result. This is not sensitive to constraints on culling rates or on total annual culls, and results are similar when the outcome being minimized is total number of animals culled or infected (social impact).

Appendix A. Derivation of the equation of motion for [SI], and the full model.

Here we demonstrate the derivation of the equation of motion for [SI] in a SEIRVC pair approximation model of FMD using a an approach similar to the one adopted by Keeling et al. (1997), Rand (1999), Bauch (2005), Ringa and Bauch (2014), and then present the model in full.

In moment closure approximations the equation of motion for any state variable, $g(t)$, is determined by summing over all events which affect the state variable. Thus the dynamics of $g(t)$ are governed governed by the master equation:

$$\frac{dg(t)}{dt} = \sum_{\epsilon \in events} r(\epsilon)\Delta g(\epsilon), \tag{A.1}$$

where $r(\epsilon)$ is the rate of event ϵ and $\Delta g(\epsilon)$ is the change this event causes in $g(t)$. As will be observed in the following illustration, at each node on the network the rates $r(\epsilon)$ and change $\Delta g(\epsilon)$ are expressed in terms of their population-averaged values as well as the deviations of those values from the expected means at a given node. The summation over each node is carried out in such a way that any significant stochasticity is incorporated in the evaluation of a state variable while the remaining stochasticity can be treated as random noise and may be discarded. We illustrate this concept below.

Before we proceed to the derivation of the equation on motion for $[SI]$, we first list all events in the model which affect this state variable:

Infection at a rate τ of a susceptible farm by its infectious neighbour (in a $S-I$ pair) converts S into E, i.e. $SI \mapsto EI$, where $\mapsto$ means 'transformed to'. This process *destroys* a $S-I$ pair. Similarly, infection at a rate τ of a susceptible farm 'from the left' in a triple $I-S-I$, i.e. $I \leftrightarrow SI$ also *destroys* a $S-I$ pair.

Transition of a farm from the exposed to the infectious state in a pair $S-E$ at a rate ν (NB: latent period is $1/\nu$) *creates* a $S-I$ pair, i.e. $SE \mapsto SI$.

Recovery of an infectious farm at a rate, σ in a pair $S-I$ implies $SI \mapsto SR$. Therefore the process *destroys* $S-I$.

Ring vaccination (defined as vaccination of exposed and susceptible farms that have links with infected farms) in the susceptible farm in a pair $S-I$, at rate ψ_r *destroys* $S-I$ by a transformation $SI \mapsto IV$. Similarly ring vaccination in the susceptible farm in a triple $I-S-I$, *destroys* $S-I$.

DC culling (defined as culling on farms neighbouring infectious farms) at a rate μ_{DC} in the susceptible farm in a pair $S-I$ and a triple $I-S-I$, similarly transforms $S-I$ into $I-C$, thereby *destroying* $S-I$.

IP culling (defined as culling on infectious farms) at a rate μ_{IP} in the infectious farm in a pair $S-I$ *destroys* $S-I$ to form $S-C$.

A recovered farm in an $I-R$ pair loses natural immunity at rate ω to *create* a $S-I$ pair.

A vaccinated farm in an $I-V$ pair loses vaccine protection at rate θ, and the process *creates* a $S-I$ pair.

Replacement of previously culled farms at a rate η *creates* $S-I$ by transforming $I-C$ into $S-I$.

The following notations will be adopted to proceed with the derivation of the equation of motion for $[SI]$:

$n_x(i)$: number of state i neighbours of a node x;

$n_{xy}(i)$: number of state i neighbours of a node x which has node y as a neighbour;

ζ_x: disease state of node x;

ζ_{xy}: disease state of an edge involving x and y.

Now we use this notation to write down the master equation for the dynamics of $[SI]$ by summing over all the events listed above:

$$\begin{aligned}\frac{d[SI]}{dt} = &\sum_{\zeta_x=S}\tau(n_x(I))(-1) + \sum_{\zeta_{xy}=SI}\tau(n_{xy}(I))(-1)\\ &+ \sum_{\zeta_x=S}\nu(n_x(E))(+1) + \sum_{\zeta_x=S}\sigma(n_x(I))(-1)\\ &+ \sum_{\zeta_x=S}\psi_r(n_x(I))(-1) + \sum_{\zeta_{xy}=SI}\psi_r(n_{xy}(I))(-1)\\ &+ \sum_{\zeta_x=R}\omega(n_x(I))(+1) + \sum_{\zeta_x=V}\theta(n_x(I))(+1)\\ &+ \sum_{\zeta_x=S}\mu_{DC}(n_x(I))(-1) + \sum_{\zeta_{xy}=SI}\mu_{DC}(n_x(I))(-1)\\ &+ \sum_{\zeta_x=S}\mu_{IP}(n_x(I))(-1) + \sum_{\zeta_x=C}\eta(n_x(I))(-1).\end{aligned}$$

The *positive* + and *negative* − signs in this formulation indicate *creation* or *destruction* of the $S-I$ pair, respectively. The next step is to replace quantities $n_x(I)$, $n_{xy}(I)$ and $n_x(E)$ by their population-averaged values (means) plus the stochastic fluctuations of those quantities from the means at the node x and pairs xy. We introduce more notations illustrate this step. Let $n(i|j)$ be the population-averaged value of $n_x(i)$ when $\zeta_x = j$ and let $n(i|jk)$ be the population-averaged value of $n_{xy}(i)$ when $\zeta_{xy} = jk$. For example here $n_{xy}(I)$ is replaced by $n(I|SI) + \rho(I|SI)$ where $\rho_{xy}(I|SI)$ represents the stochastic fluctuation from the mean. The resulting expression is then simplified by taking out constants such as $n(I|SI)$ and the model parameters out of the sums and further noting that terms such as $\sum_{\zeta_x=S}\rho_x(I|S)$ which represent fluctuations are zero by definition. Furthermore the following identities (which apply to all network types):

$$n(i|jk) = \frac{[ijk]}{[jk]};\ n(i|ji) = 1 + \frac{[iji]}{[ji]};\ n(i|j) = \frac{[ij]}{[j]} \text{ and } n(i|i) = 1 + \frac{[ii]}{[i]},$$

enable us to write the equation of motion for $[SI]$ as

$$\begin{aligned}\frac{d[SI]}{dt} = &-\tau([ISI]+[SI]) + \nu[SE] - \sigma[SI] - \psi_r([SI]+[ISI])\\ &- \psi_p[SI] + \omega[IR] + \theta[IV] - \mu_{DC}([SI]+[ISI])\\ &- \mu_{IP}[SI] + \eta[IC].\end{aligned}$$

Since farms are distributed on a random network in which the neighbourhood size is assumed to obey a Poisson distribution, and also allows for conditional independence in neighbour status, third order correlations take the form

$$n(i|jk) = n(i|j) \text{ and } n(i|ji) = 1 + n(i|j).$$

Note that now we can substitute the identities stated earlier to write triples in terms of pairs and singletons:

$$[ijk] = \frac{[ij][jk]}{[j]} \text{ and } [iji] = \frac{[ij]^2}{[j]}.$$

Below is the full system of our pair approximations model.

A.1. The model

$$\begin{aligned}
\frac{d[S]}{dt} &= -\tau[SI] - \psi_r[SI] - \psi_p[S] + \omega[R] + \theta[V]\\ &\quad - \mu_{DC}[SI] + \eta[C]\\
\frac{d[E]}{dt} &= \tau[SI] - \nu[E] - \psi_r[EI] - \mu_{DC}[EI]\\
\frac{d[I]}{dt} &= \nu[E] - \sigma[I] - \mu_{IP}[I]\\
\frac{d[R]}{dt} &= \sigma[I] - \omega[R]\\
\frac{d[V]}{dt} &= \psi_r[SI] + \psi_r[EI] + \psi_p[S] - \theta[V]\\
\frac{d[C]}{dt} &= \mu_{DC}[SI] + \mu_{DC}[EI] + \mu_{IP}[I] - \eta[C]\\
\frac{d[SS]}{dt} &= -2\tau[SSI] - 2\psi_r[SSI] - 2\psi_p[SS] + 2\omega[SR]\\ &\quad + 2\theta[SV] - 2\mu_{DC}[SSI] + 2\eta[SC]\\
\frac{d[SE]}{dt} &= -\tau([ISE]-[SSI]) - \nu[SE] - \psi_r([ISE]\\ &\quad + [SEI]) - \psi_p[SE] + \omega[ER] + \theta[EV]\\ &\quad - \mu_{DC}([ISE]+[SEI]) + \eta[EC]\\
\frac{d[SI]}{dt} &= -\tau([ISI]+[SI]) + \nu[SE] - \sigma[SI]\\ &\quad - \psi_r([SI]+[ISI]) + \omega[IR] + \theta[IV]\\ &\quad - \mu_{DC}([SI]+[ISI]) - \mu_{IP}[SI] + \eta[IC]\\
\frac{d[SR]}{dt} &= -\tau[ISR] + \sigma[SI] - \psi_r[ISR] - \psi_p[SR]\\ &\quad - \omega([SR]-[RR]) + \theta[RV] - \mu_{DC}[ISR] + \eta[RC]\\
\frac{d[SV]}{dt} &= -\tau[ISV] - \psi_r([ISV]-[SSI]-[SEI])\\ &\quad - \psi_p([SV]-[SS]) + \omega[RV] + \theta([VV]-[SV])\\ &\quad - \mu_{DC}[ISV] + \eta[VC]\\
\frac{d[SC]}{dt} &= \mu_{DC}([SSI]+[SEI]-[ISC]) + \mu_{IP}[SI] - \eta[SC] + \eta[CC]\\
\frac{d[EE]}{dt} &= 2\tau[ESI] - 2\nu[EE] - 2\psi_r[EEI] - 2\mu_{DC}[EEI]\\
\frac{d[EI]}{dt} &= \tau([ISI]+[SI]) + \nu([EE]-[EI]) - \sigma[EI] - \psi_r([EI]\\ &\quad + [IEI]) - \mu_{DC}([EI]+[IEI]) - \mu_{IP}[EI]\\
\frac{d[ER]}{dt} &= \tau[ISR] - \nu[ER] + \sigma[EI] - \psi_r[IER]\\ &\quad - \omega[ER] - \mu_{DC}[IER]\\
\frac{d[EV]}{dt} &= \tau[ISV] - \nu[EV] - \psi_r([IEV]-[ISE]-[EEI])\\ &\quad + \psi_p[SE] - \theta[EV] - \mu_{DC}[IEV]\\
\frac{d[EC]}{dt} &= \mu_{DC}([ISE]+[EEI]-[IEC]) + \mu_{IP}[EI] - \eta[EC]\\
\frac{d[II]}{dt} &= 2\nu[EI] - 2\sigma[II] - 2\mu_{IP}[II]\\
\frac{d[IR]}{dt} &= \sigma([II]-[IR]) + \nu[ER] - \omega[IR] - \mu_{IP}[IR]\\
\frac{d[IV]}{dt} &= -\sigma[IV] + \nu[EV] + \psi_r([SI]+[ISI]+[EI]+[IEI])\\ &\quad - \theta[IV] - \mu_{IP}[IV]\\
\frac{d[IC]}{dt} &= \mu_{DC}([ISI]+[SI]+[IEI]+[EI]) - \mu_{IP}[IC] - \eta[IC]\\
\frac{d[RR]}{dt} &= 2\sigma[IR] - 2\omega[RR]\\
\frac{d[RV]}{dt} &= \sigma[IV] + \psi_r([ISR]+[IER]) + \psi_p[SR]\\ &\quad - \omega[RV] - \theta[RV]\\
\frac{d[RC]}{dt} &= \mu_{DC}([ISR]+[IER]) + \mu_{IP}[IR] - \eta[RC]\\
\frac{d[VV]}{dt} &= 2\psi_r([IEV]+[ISV]) + 2\psi_p[SV] - 2\theta[VV]\\
\frac{d[VC]}{dt} &= \mu_{DC}([ISV]+[IEV]) + \mu_{IP}[IV] - \eta[VC]\\
\frac{d[CC]}{dt} &= 2\mu_{DC}([ISC]+[IEC]) + 2\mu_{IP}[IC] - 2\eta[CC]
\end{aligned} \tag{A.2}$$

The factor 2 in the equations of motion pairs of the form $[XX]$ comes from the counting convention of same-status pairs such that, e.g. $[II]$ denotes twice the number of infected-infected pairs (Bauch, 2005). We note that most equations of motion for pairs involve triples (terms of the form $[XYZ]$). As described in the Introduction, in order to apply numerical methods to solve this system we need to express these triples in terms of pairs and singletons. Here we assume conditional independence of neighbours of a farm and a

Poisson neighbourhood size so that triples are approximated by the Poisson OPA:

$$[XYZ] = \frac{[XY][YZ]}{[Y]}. \tag{A.3}$$

Note that farms X and Z are only connected through farm Y.

Appendix B. Derivation of the basic reproduction number

Here we present the derivation of the basic reproduction number for our pair approximation model of foot and mouth disease.

At the initial stage of the infection an outbreak is expected to take off in the numbers of exposed, $[E]$ and infectious, $[I]$ farms increase. That is an epidemic is expected if $(d/dt)[E]+(d/dt)[I]>0$ or the disease will to die out if $(d/dt)[E]+(d/dt)[I]<0$. Substituting the equations of motion for $[E]$ and $[I]$ from Eq. (A.1) into the either of the inequalities above shows that the disease will spread if

$\tau[SI]-(\psi_r+\mu_{DC})[EI]-(\sigma+\mu_{IP})[I]>0$.

The definition of the correlation between any two farms given by Eq. (1) implies that $[SI]$ and $[EI]$ in the expression above can be written in terms of the correlation between susceptible and infectious farms, and between the exposed and infectious farms, respectively, so that the condition under which the disease will spread is now

$$\tau n\tfrac{[S][I]}{N}C_{SI}-(\psi_r+\mu_{DC})n\tfrac{[E][I]}{N}C_{EI}-(\sigma+\mu_{IP})[I]>0.$$

We divide this inequality by $[I]$ and use the convention that at the beginning of an epidemic (initial inoculation) there is only one or very few infected farms such that almost the entire population is susceptible, i.e. $[S]\approx N$, to rewrite the condition for the spread of the disease as

$$\tau nC_{SI}-(\psi_r+\mu_{DC})n\tfrac{[E]}{N}C_{EI}-(\sigma+\mu_{IP})>0 \text{ or}$$

$$\frac{\tau nC_{SI}}{(\psi_r+\mu_{DC})n([E]/N)C_{EI}+(\sigma+\mu_{IP})}>1.$$

The left hand side of the expression above is essentially the basic reproduction number. That is the basic reproduction number is a function of the transmission rate, the average neighbourhood size, vaccination, culling, correlation between susceptible and infectious farms and correlation between exposed and infectious farms:

$$R_0=\frac{\tau nC_{SI}}{(\psi_r+\mu_{DC})n([E]/N)C_{EI}+(\sigma+\mu_{IP})}. \tag{B.1}$$

Note that in the absence of control measures Eq. (B.1) transforms to a simpler expression of the basic reproduction number:

$$R_0=\tfrac{\tau nC_{SI}}{\sigma}.$$

While in the case of mean-field equations, C_{SI} and $([E]/N)C_{EI}$ are assumed to remain constant over time, here these correlations are variables and their critical values are crucial in the derivation of the basic reproduction number (Bauch, 2005; Parham et al., 2008). For instance, at the beginning of an epidemic when almost the entire population is susceptible, then $C_{SI}\approx 1$. C_{SI} decreases as more farms become infected and the subsequent clustering of infected farms creates a situation where the infection is 'wasted', resulting in reduction of the infection rate, and at this point the epidemic may die out if there are no susceptible farms in the neighbourhood to acquire and transmit the disease further. This point is a local minimum of C_{SI}, and is denoted by C^*_{SI}. Thus the disease dynamics at this point will determine whether or not the disease will spread. This value is obtained by solving $(d/dt)C_{SI}=0$. In a similar manner the basic reproduction number is defined by the critical value $(([E]/N)C_{EI})^*$, obtained by solving $(d/dt)([E]/N)C_{EI}=0$. Therefore we need to evaluate C^*_{SI} and $(([E]/N)C_{EI})^*$ and substitute them into Eq. (B.1) to give an explicit form of the basic reproduction number.

First we evaluate C^*_{SI}. The equation of motion for the the correlation between susceptible and infectious farms is given by

$$\tfrac{d}{dt}C_{SI}=\tfrac{N}{n}\tfrac{1}{[S][I]}\tfrac{d}{dt}[SI]+C_{SI}(-\tfrac{1}{[I]}\tfrac{d}{dt}[I]-\tfrac{1}{[S]}\tfrac{d}{dt}[S]).$$

Substituting the equation of motion for $[SI]$ from Eq. (A.2) into the equation above, applying the Poisson OPA (Eq. (A.3)) to express terms involving triples as pairs and singletons and expressing pairs in terms of their correlation functions, show that the first term of the equation of motion for C_{SI} is given by

$$\begin{aligned}\tfrac{N}{n}\tfrac{1}{[S][I]}\tfrac{d}{dt}[SI]=&-\tau n\tfrac{[I]}{N}C_{SI}^2-\tau C_{SI}+\nu\tfrac{[E]}{[I]}C_{SE}-\sigma C_{SI}-\psi_r n\tfrac{[I]}{N}C_{SI}^2\\&-\psi_r C_{SI}-\psi_p C_{SI}-\mu_{DC}n\tfrac{[I]}{N}C_{SI}^2\\&-\mu_{DC}C_{SI}-\mu_{IP}C_{SI}+\omega\tfrac{[R]}{[S]}C_{IR}+\theta\tfrac{[V]}{[S]}C_{IV}+\eta\tfrac{[C]}{[S]}C_{IC}.\end{aligned}$$

The remaining terms of the equation of motion for C_{SI} are

$$\begin{aligned}C_{SI}\left(-\tfrac{1}{[I]}\tfrac{d}{dt}[I]-\tfrac{1}{[S]}\tfrac{d}{dt}[S]\right)=&-\nu\tfrac{[E]}{[I]}C_{SI}+\sigma C_{SI}\\&+\mu_{IP}C_{SI}+\tau n\tfrac{[I]}{N}C_{SI}^2+\psi_r n\tfrac{[I]}{N}C_{SI}^2+\psi_p C_{SI}\\&+\mu_{DC}n\tfrac{[I]}{N}C_{SI}^2-\omega\tfrac{[R]}{[S]}C_{IR}-\theta\tfrac{[V]}{[S]}C_{IV}-\eta\tfrac{[C]}{[S]}C_{IC}.\end{aligned}$$

Therefore

$$\tfrac{d}{dt}C_{SI}=-\left(\tau+\psi_r+\mu_{DC}+\nu\tfrac{[E]}{[I]}\right)C_{SI}+\nu\tfrac{[E]}{[I]}C_{SE}.$$

We use a convention also adopted by Rand (1999), Parham et al. (2008), Keeling et al. (1997), that on a network where nodes X and Z in a triple $X-Y-Z$ are conditionally independent, i.e. no triangles, then when a susceptible farm becomes exposed, this newly exposed farm inherits the neighbourhood of the susceptible, and this means C_{SE} is related to C_{SI} such that $C_{SE}\approx((n-1)/n)C_{SS}$. However at the beginning of an infection almost all farms are susceptible, therefore $C_{SS}\approx 1$, so that $C_{SE}\approx((n-1)/n)$ Similar arguments can be made to approximate $([E]/[I])$. That is the process of a farm moving from the exposed to the infectious state implies that the farm now inherits a fraction $(n-1)/n$ of the neighbourhood it had previously so that $([E]/[I])\approx n-1/n$.

Therefore the equation of motion for C_{SI} now becomes

$$\tfrac{d}{dt}C_{SI}=-\left(\tau+\psi_r+\mu_{DC}+\nu\tfrac{n-1}{n}\right)C_{SI}+\nu\tfrac{(n-1)^2}{n^2}$$

and the value of C_{SI} associated to R_0 is

$$C^*_{SI}=\frac{\nu(n-1)^2}{n[(n-1)\nu+(\tau+\psi_r+\mu_{DC})n]}.$$

Another critical value of the basic reproduction number $(([E]/N)C_{EI})^*$ is obtained by solving

$$\frac{d}{dt}\frac{[E]C_{EI}}{N}=\frac{1}{n}\left(-\frac{[EI]}{[I]^2}\frac{d}{dt}[I]+\frac{1}{[I]}\frac{d}{dt}[EI]\right).$$

Substituting the equations of motion for $[I]$ and $[EI]$ and employing similar assumptions to those applied in the derivation of C^*_{SI} above, and further noting that in a large population the initial disease dynamics are characterized by very small values of terms such as $([I]/N)C_{SI}^2$ (i.e. $([I]/N)C_{SI}^2\to 0$ as $N\to\infty$), we show that the equation

of motion for $([E]/N)C_{EI}$ can be written as

$$\frac{d}{dt}\left(\frac{[E]}{N}C_{EI}\right) = \tau C_{SI} - \nu\frac{n-1}{n}\left(\frac{[E]}{N}C_{EI}\right) + \nu\frac{n-1}{n}\left(\frac{[E]}{N}C_{EE}\right) - \nu\left(\frac{[E]}{N}C_{EI}\right) - \psi_r\left(\frac{[E]}{N}C_{EI}\right) - \psi_r q\left(\frac{[E]}{N}C_{EI}\right) - \mu_{DC}\left(\frac{[E]}{N}C_{EI}\right) - \mu_{DC}q\left(\frac{[E]}{N}C_{EI}\right),$$

where $q = [EI]/[E]$. We carried out a separate study to show that q varies with the structure of the network. Furthermore we argue that when all correlations are at their quasi-equilibria then $([E]/N)C_{EI}$ (proportional to the expectation of an exposed farm given that there is an infectious farm within its neighbourhood) will always be much higher than $([E]/N)C_{EE}$ (proportional to the expectation of finding an exposed farm given that an exposed farm resides nearby). That is there is a higher probability of becoming becoming infected when nearest neighbours are infectious. This allows us to approximate the equation of motion for $([E]/N)C_{EI}$ by

$$\frac{d}{dt}\left(\frac{[E]}{N}C_{EI}\right) = \tau C_{SI} - \left(\nu\frac{n-1}{n} + \nu + \psi_r + \psi_r q + \mu_{DC} + \mu_{DC}q\right)\left(\frac{[E]}{N}C_{EI}\right)$$

Therefore

$$\left(\frac{[E]}{N}C_{EI}\right)^* = \frac{\tau n C_{SI}^*}{(2n-1)\nu + n(q+1)(\psi_r + \mu_{DC})}.$$

We simplify this expression further by replacing C_{SI}^* by its explicit form derived above, and write

$$\left(\frac{[E]}{N}C_{EI}\right)^* = \frac{\tau\nu(n-1)^2}{[(n-1)\nu + (\tau + \psi_r + \mu_{DC})n][(2n-1)\nu + n(q+1)(\psi_r + \mu_{DC})]}.$$

In summary the expression of the basic reproduction number for our model is given by

$$R_0 = \frac{\tau n C_{SI}^*}{(\psi_r + \mu_{DC})n\left(([E]/N)C_{EI}\right)^* + (\sigma + \mu_{IP})},$$

where C_{SI}^* and $(([E]/N)C_{EI})^*$ are as presented above.

Appendix C. Supplementary data

Supplementary data associated with this article can be found, in the online version, at http://dx.doi.org/10.1016/j.epidem.2014.09.008.

References

Alonso, A., Martins, M.A., Gommes, M.D., Allende, R., Sondahl, M.S., 1992. Foot and mouth disease viral typing by complement fixation and enzyme-linked immunosorbent assay monovalent and polyvalent antisera. J. Vet. Diagn. Invest. 4, 249–253.

Anderson, E.C., Anderson, J., Doughty, J., 1974. The foot and mouth disease subtype variants in Kenya. J. Hyg. (London) 72 (2), 237–244.

Baipoledi, E.K., Matlho, G., Letshwenyo, M., Chimbombi, M., Adom, E.K., Raborokgwe, M.V., Hyera, J.M.K., 2004. Re-emergence of foot and mouth disease in Botswana. Vet. J. 168, 93–99.

Barteling, S.J., 2002. Development and performance of inactivated vaccines against foot and mouth disease. Rev. Sci. Tech. 21 (3), 577–588.

Bauch, C.T., 2005. The spread of infectious diseases in spatially structured populations: an invasory pair approximation. Math. Biosci. 198, 217–237.

Bauch, C.T., Galvani, A.P., 2003. Using network models to approximate spatial point-process models. Math. Biosci. 184, 101–114.

Belsham, G.J., Jamal, S.M., Tkornehoj, K., Botner, A., 2011. Rescue of foot-and-mouth disease viruses that are pathogenic for cattle from preserved viral RNA samples. PLoS ONE 6 (1), 1–10.

Brauer, F., 2006. Some simple epidemic models. Math. Biosci. Eng. 3 (1), 1–15.

Bruckner, G., Saraiva-Vieira, V.E., 2010. OIE strategy for the control and eradication of foot and mouth disease at regional and global level. Conf. OIE, 187–198.

Cruz-Aponte, M., McKiernan, E.C., Herrera-Valdez, M.A., 2011. Mitigating effects of vaccination on influenza outbreaks given constraints in stockpile size and daily administration capacity. BMC Infect. Dis. 11 (207).

Davies, G., 2002. Foot and mouth disease. Res. Vet. Sci. 73, 195–199.

Depa, P.M., Dimri, U., Sharma, M.C., Tiwari, R., 2012. Update on epidemiology and control of foot and mouth disease: a menace to international trade and global animal enterprise. Vet. World 5 (11), 694–704.

Ding, Y., Chen, H., Zhang, J., Zhou, J., Ma, L., Zhang, L., Gu, Y., Liu, Y., 2013. An overview of control strategy and diagnostic technology for foot-and-mouth disease in China. Virol. J. 10 (78), 1–6.

Dion, E., Van Schalkwyk, L., Lambin, E.F., 2011. The landscape epidemiology of foot-and-mouth disease in South Africa: a spatially explicit multi-agent simulation. Ecol. Model. 222 (13), 2059–2072.

Doel, T.R., 1996. Natural and vaccine-induced immunity to foot and mouth disease: the prospects for improved vaccines. Rev. Sci. Tech. 15 (3), 883–911.

Evans, B., 2006. The social and political impact of animal diseases. Vet. Ital. 42 (4), 399–406.

Ferguson, N.M., Donnelly, C.A., Anderson, R.M., 2001. The foot and mouth epidemic in Great Britain: pattern of spread and impact of interventions. Science 292, 1155–1160.

Ferguson, N.M., Donnelly, C.A., Anderson, R.M., 2001. Transmission intensity and impact of control policies on the foot and mouth epidemic in Great Britain. Nature 413 (6855), 542–548.

Garnett, G.P., 2002. An introduction to mathematical models in sexually transmitted disease epidemiology. Sex Transm. Infect. 78, 7–12.

Grubman, M.J., Baxt, B., 2004. Foot and mouth disease. Clin. Microbiol. Rev. 17 (2), 465–493.

Grubman, M.J., Baxt, B., 2004. Foot-and-mouth disease. Clin. Microbiol. Rev. 17 (2), 465–493.

Hansen, E., Day, T., 2011. Optimal control of epidemics with limited resources. J. Math. Biol. 62, 432–451.

James, A.D., Rushton, J., 2002. The economics of foot and mouth disease. Rev. Sci. Tech. 21 (3), 637–644.

Keeling, M.J., Rand, D.A., Morris, A.J., 1997. Correlation models for childhood epidemics. Proc. R. Soc. Lond. B 264, 1149–1156.

Keeling, M.J., Woolhouse, M.E.J., May, R.M., Davies, G., Grenfel, B.T., 2003. Modeling vaccination strategies against foot and mouth disease. Nature 421, 136–142.

Keeling, M.J., Woolhouse, M.J., Shaw, D.J., Matthews, L., Chase-Topping, M., Haydon, D.T., Cornell, S.J., Kappey, J., Wilesmith, J., Granfell, B.T., 2001. Dynamics of the 2001 UK foot and mouth disease: stochastic dispersal in a heterogeneous landscape. Science 294 (5543), 813–817.

Kitching, P., Hammond, J., Jeggo, M., Charleston, B., Paton, D., Rodriguez, L., Heckert, R., 2007. Global FMD control: is it an option? Vaccine 25 (30), 5660–5664.

Kitching, R.P., 1998. recent history of foot and mouth disease. J. Comp. Pathol. 118, 89–108.

Kobayashi, M., Carpenter, T.E., Dickey, B.F., Howitt, R.E., 2007. A dynamic optimal disease control model for foot-and-mouth-disease: Ii. model results and policy implications. Prev. Vet. Med. 79, 274–286.

Mardones, F., Perez, A., Sanchez, J., Alkhamis, M., Carpenter, T., 2010. Parameterization of the duration of infection stages of serotype o foot-and-mouth disease virus: an analytical review and meta-analysis with application to simulation models. Vet. Res. 41 (4), 45.

Mokopasetso, M., Derah, N., 2005. Recent outbreaks of foot and mouth disease in Botswana and Zimbabwe., pp. 8–12.

Mushayabasa, S., Bhunu, C.P., Dhlamini, M., 2011. Impact of vaccination and culling on controlling foot and mouth disease: a mathematical modeling approach. World J. Vaccines 1, 156–161.

Neilan, R.M., Lenhart, S., 2010. An introduction to optimal control with an application in disease modeling. Am. Math. Soc. 75, 67–81.

Parham, P.E., Singh, B.K., Ferguson, N.M., 2008. Analytical approximation of spatial epidemic models of foot and mouth disease. Theor. Popul. Biol. 72, 349–368.

Patterson, T.S., 2001. Constraints: an integrated viewpoint. Illuminare 7 (1), 30–38.

Pharo, H.J., 2002. Foot and mouth disease: an assessment of the risks facing new zealand. N. Z. Vet. J. 50 (2), 46–55.

Porphyre, T., Auty, H.K., Tildesley, M.J., Gunn, G.J., Woolhouse, M.E.J., 2013. Vaccination against foot-and-mouth disease: do initial conditions affect its benefit? PLoS ONE 8 (10), e77616.

Rand, D.A., 1999. Correlation equations and pair approximations for spatial ecologies. CWI Q. 12 (3 and 4), 329–368.

Rico-Ramirez, V., Napoles-Rivera, F., Gonzalez-Alatorre, G., Diwekar, U.M., 2010. Stochastic optimal control for the treatment of a pathogenic disease. Comput. Aided Chem. Eng. 28, 217–222.

Ringa, N., Bauch, C.T., 2014. Dynamics and control of foot and mouth disease in endemic countries: a pair approximation model. J. Theor. Biol. 357, 150–159.

Roy, S., McElwain, T.F., Wan, Y., 2011. A network control theory approach to modeling and optimal control of zoonoses: case study of brucellosis transmission in sub-saharan africa. PLoS. Negl. Trop. Dis. 5 (10), e1259.

Rweyemamu, M., 1984. Foot and mouth disease control strategies in Africa. Prev. Vet. Med. 2, 329–340.

Rweyemamu, M., 2002. Global perspective for foot and mouth disease control. Rev. Sci. Tech. 21, 765–773.
Tildesley, M.J., Bessell, P.R., Keeling, M.J., Woolhouse, M.E.J., 2009. The role of pre-emptive culling in the control of foot-and-mouth disease. Proc. R. Soc. B 276 (1671), 3236–3248, 22.
Tildesley, M.J., Savill, N.J., Shaw, D.J., Deardon, R., Brooks, S.P., Woolhouse, M.E., Grenfell, B.T., Keeling, M.J., 2006. Optimal reactive vaccination strategies for a foot-and-mouth outbreak in the UK. Nature 440 (7080), 83–86.
Wernery, U., Kinne, J., 2012. Foot and mouth disease and similar virus infections in Camelids: a review. Rev. Sci. Tech. 31 (3), 907–918.